




Investigation on the effect of Potassium on the structural, optical and thermal properties of the L-Threonine Cadmium acetate: Elucidation of organo-cadmium compound for dielectric filters

M. Abila Jeba Queen^{1,*} , K. C. Bright², and P. Aji Udhaya¹

¹Department of Physics, Holy Cross College (Autonomous), Nagercoil 629004, India

²Department of Physics, Mar Ivanios College (Autonomous), Thiruvananthapuram, Kerala 695015, India

Received: 22 April 2022

Accepted: 7 December 2022

© The Author(s), under exclusive licence to Springer Science+Business Media, LLC, part of Springer Nature 2023

ABSTRACT

In this study, the metal cation potassium-doped organo-cadmium compound has been prepared from the chemical reaction between amino acid and metal complexes by slow evaporation technique. The resultant compound belongs to monoclinic crystal system with two ligancies and a two-fold configuration. The presence of potassium metal via the organo-cadmium compound has been estimated using energy-dispersive X-ray analysis. The optical characteristics and bandgap edges calculations show that it is a good insulator for energy storage applications. The integration of potassium causes disruption within the parent compound's host lattice, resulting in an increase in static permittivity. Furthermore, the influence of potassium increases Fermi velocity, Fermi temperature, and plasma energy, according to theoretical studies. Potassium also improves thermal stability and magnetic properties. Using a Neodymium-doped Yttrium Aluminum Garnet (Nd-YAG) laser, the crystal's nonlinear optical property was investigated.

1 Introduction

Nowadays, the developments of new organometallic compounds with excellent optical and dielectric properties are attracted toward the researchers due to its biocompatibility and sensor applications [1]. Organometallic species belong to the general class of coordination compound and they have synthesized with a wide variety of organic substrate [2].

Nonlinear optical organometallic crystals with higher Second Harmonic Generation (SHG) efficiency and Ultra Violet (UV)-Visible transparency are necessary for numerous device applications [3, 4]. In this regard, amino acid organometallic crystals are important candidates for NLO applications because of its non-centrosymmetric and zwitterionic structure. The material's superior optical, thermal, and magnetic stabilities lead to their extensive use in a

Address correspondence to E-mail: jeba.abi@gmail.com

number of device applications [5]. Because of its higher melting temperature, higher density, and lower strength, potassium acetate, an essential macromineral, has been used in the paper and textile industries as a de-icer, fire extinguisher, preservative, acid regulator, catalyst, and softening agent [6]. L-threonine cadmium acetate monohydrate (LTCA), a biocompatible solid-state material, has wide industrial applications such as binder, additives, resist humid atmosphere [7–9].

Organometallic compound L-threonine cadmium acetate monohydrate (LTCA) has been successfully crystallized by slow evaporation technique at room temperature and its detailed structural parameters are reported [10]. Initial interest in the structural property of the compound was extended to investigate various properties like optical, dielectric, thermal, and a nonlinear optical property which was reported earlier [11]. LTCA crystal experiences lower UV cutoff wavelength and good dielectric material and exhibits diamagnetic behavior. Followed by this, we recently reported the effect of zinc and lead as a dopant on the structural, optical, and magnetic properties of L-threonine cadmium acetate crystal [12]. In the present work, our aim is to give a brief description of potassium (K)-doped LTCA crystal with improved optical, thermal, dielectric, magnetic, and nonlinear optical properties.

2 Materials and methods

2.1 Synthesis

Potassium-doped L-threonine cadmium acetate monohydrate has been prepared from biomass as the L-threonine and metal organic frame as the cadmium acetate dihydrate in a stoichiometric proportion. This is followed by doping 0.3 mol percentage of potassium cation by the treatment of potassium acetate. Deionized water is utilized as a solvent during the series of chemical reactions. The resulting solution is mechanically stirred and then continuously heated to 40 °C until it becomes dry. After cooling, a homogeneous solution was prepared by thoroughly dissolving the mixture in the solvent. The prepared solution was filtered and allowed for slow evaporation. After 25–35 days, a good-quality crystal of potassium-doped LTCA was harvested as shown in Fig. 1.

2.2 Characterization

The X-ray diffractometer system with the X'Pert pro family of multipurpose PAN analytical diffractometer was used to determine the crystal structure of the grown potassium-doped crystal. Continuous scanning was employed in the 10–70° range with a scan time of 10.16 s. The crystalline planes were determined using the INDEX software package. The lattice parameters and crystallographic axes were computed using a Bruker Kappa APES II single-crystal X-ray diffractometer with MoK α ($\lambda = 0.71073$ Å) radiation. Elemental confirmations were carried out using the EDAX analysis OXFORD XMX N model.

The transmittance spectrum has been recorded using UV spectrophotometer (ELICO) for the grown crystal. The optical bandgap (E_g) of K⁺ ion-doped LTCA at the lower cutoff wavelength (λ) is evaluated using the relation [13],

$$E_g = \frac{hc}{\lambda} \quad (1)$$

where h is the Planck's constant and c is the velocity of light. Furthermore, the position of the valance and conduction band [14] of the potassium-doped compound can be determined using the relations as follows;

$$E_{(CB)} = \chi - E^c - 0.5E_g \quad (2)$$

$$E_{(VB)} = E_{(CB)} + E_g \quad (3)$$

χ represents the absolute electronegativity of the compound, calculated as the arithmetic mean of electron affinity and first ionization energy. E^c denotes the energy of free electrons on the hydrogen scale, i.e., 4.5 eV, where $E_{(CB)}$ is the band edge

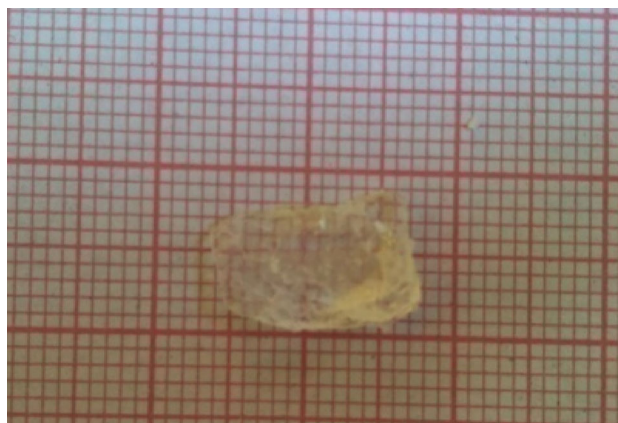


Fig. 1 Grown K⁺ ion-doped LTCA

position of the valance band, $E_{(VB)}$ is the band edge position of the conduction band.

Refractive index is considered as the most important optical property of the crystal. In order to determine the refractive index of the crystal, the absorption coefficient (α), extinction coefficient (K), and reflectance (R) were evaluated using the following relations [15–17];

$$\alpha = \frac{2.303 \times \log \frac{1}{T}}{t} \tag{4}$$

$$K = \frac{\lambda \alpha}{4\pi} \tag{5}$$

$$R = \frac{\exp(-\alpha t) + \sqrt{\exp(-\alpha t)T - \exp(-3\alpha t)T + \exp(-2\alpha t)T^2}}{\exp(-\alpha t) + \exp(-2\alpha t)T} \tag{6}$$

where t is the thickness of the crystal and T is the transmittance value.

Therefractiveindex, $n = -(R + 1) + \frac{2\sqrt{R}}{R - 1}$ (7)

Furthermore, the electrical susceptibility (χ_c) is obtained using the following relation [18],

$$\chi_c = \frac{n^2 - K^2 - \epsilon_0}{4\pi} \tag{8}$$

ϵ_0 is the dielectric constant in the absence of free charge carriers. From the calculated bandgap, the electronic polarization (α^1) can be calculated using the relation,

$$\alpha^1 = \left[1 - \sqrt{\frac{E_g}{4.06}} \right] \times \left[\frac{M}{\rho} \right] 0.396 \times 10^{-24} \text{cm}^3 \tag{9}$$

Dielectric measurements such as capacitance value and dielectric losses were measured using an LCR impedance analyzer in the range of 1 kHz to 2 MHz. Using the dielectric results, some theoretical calculations were performed for K^+ -doped LTCA crystal to find the Penn gap, Fermi gap, polarization, etc., [19, 20].

The valence electron plasma energy is

$$\hbar\omega_p = 28.8\sqrt{(Z\rho/M)} \tag{10}$$

where Z is the total number of valence electrons, ρ is the density, and M is the molecular weight of the potassium-doped LTCA crystal. Penn gap (E_p) and Fermi gap (E_F) determines the conductivity of electrons [21] and the velocity of electrons taking part in the ordinary conduction process, respectively.

$$E_p = \frac{\hbar\omega_p}{(\epsilon_\infty - 1)^{1/2}} \tag{11}$$

$$E_F = 0.2948(\hbar\omega_p)^{4/3} \tag{12}$$

Fermi velocity (V_F) and Fermi temperature (T_F) were obtained using the following relation:

$$V_F = \sqrt{\frac{2E_F}{m}} \tag{13}$$

$$T_F = \frac{k}{E_F} \tag{14}$$

where m is the mass of the electron and k is the Boltzmann constant. Polarizability (P) is calculated using the Clausius Mossotti relation [21],

$$P = \frac{3M}{4\pi N_a \rho} \left[\frac{\epsilon_\infty - 1}{\epsilon_\infty + 2} \right] \tag{15}$$

The polarizability, P , using Penn gap analysis is,

$$P = \left[\frac{(\hbar\omega_p)^2 S_0}{(\hbar\omega_p)^2 S_0 + 3E_p^2} \right] \times \left[\frac{M}{\rho} \right] \times 0.396 \times 10^{-24} \text{cm}^3 \tag{16}$$

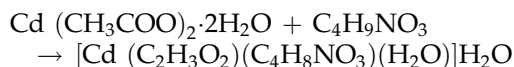
where S_0 is the constant for a particular material and is given by

$$S_0 = 1 - \left[\frac{E_p}{4E_F} \right] + \frac{1}{3} \left[\frac{E_p}{4E_F} \right]^2 \tag{17}$$

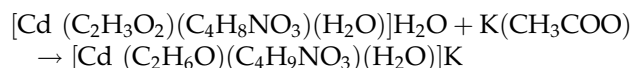
To fully understand the thermal stability and chemical degradation of the produced crystals, thermo gravimetric (TG/DTA) measurements were carried out. The measurements were made using a Perkin Elmer STA 6000 thermal analyser instrument. Magnetic behavior of the crystal was identified using vibrating sample magnetometry (VSM) analysis. One of the crucial aspects of nonlinear optics is the second harmonic generation (SHG). The efficiency of the SHG was assessed using a modified Kurtz and Perry method.

3 Results and discussion

The host organometallic compound L-threonine cadmium acetate monohydrate has been crystallized by reacting L-threonine with cadmium acetate dihydrate as follows:



LTCA molecules experience hydrophilic nature, in which the solvent inclusions are considerable in an organometallic compound. K^+ ion-doped LTCA crystallized in the chemisorption reaction of potassium acetate and L-threonine cadmium acetate monohydrate.



The powder X-ray diffraction spectrum of K^+ ion-doped LTCA (Fig. 2) confirms that the molecules are found to be in crystalline nature due to the presence of sharp peaks. Compared to the XRD pattern of pure LTCA, K^+ ion-doped LTCA shows the only variation in the peak intensities, which is mainly due to the interaction of potassium ions on the crystal system. Furthermore, the sharp peak was recorded at $2\theta = 16.73^\circ$ with maximum intensity of 916 counts in the (0 0 2) plane.

Single-crystal XRD study reveals that K^+ ion-doped LTCA belongs to monoclinic crystal system with $a = 5.846 \text{ \AA}$, $b = 8.898 \text{ \AA}$, $c = 10.758 \text{ \AA}$, $\alpha = 90^\circ$, $\beta = 91.84^\circ$, $\gamma = 90^\circ$, volume = 559 \AA^3 , and space group P2_1 . Compared to pure LTCA [11], $\alpha = 90^\circ$, $\beta = 90^\circ$, and $\gamma = 91.916^\circ$, K^+ ion-doped LTCA shows the distinction in the lattice parameters and

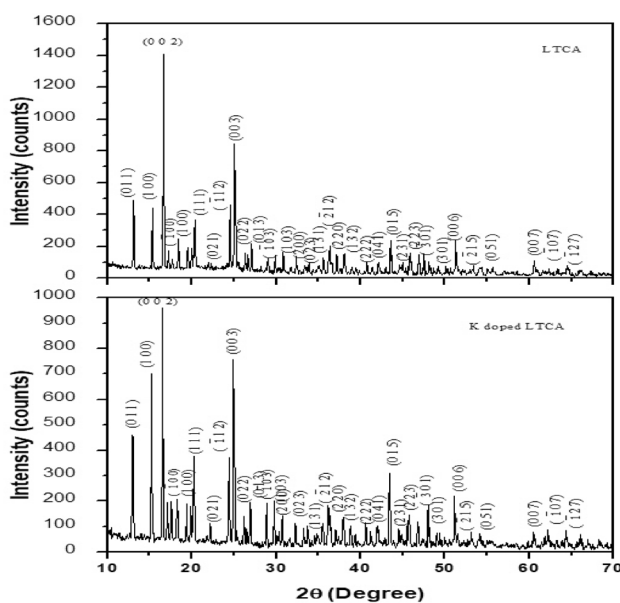


Fig. 2 XRD pattern of pure and K^+ ion-doped LTCA

crystallographic axes due to the perturbation arising in the host monoclinic crystal lattice. As a result, the variation in the secondary bond length and bond angles arises. In LTCA molecular structure, the metal cadmium was bounded with acetate, threonate, and water environments; in addition to that, incorporation of potassium tends to produce potassium metal linkage through acetate within the molecules [10]. Due to doping, K^+ ions replace the cation in the crystal lattice of LTCA leading to the formation of K^+ ion-doped LTCA. Such replacement causes distortion in the crystalline lattice. Furthermore, the calculated ionic radius of a cation (r_c) and anion (r_a) presents in the complex is 0.95138 \AA and 20.3145 \AA , respectively. The ratio of cation to anion radius r_c/r_a is found to be 0.0468; as a result, the K^+ ion-doped LTCA crystal exhibits linear two-fold configuration with two ligancies [22].

Moreover, X-ray diffraction shows small variation in lattice parameters on adding dopants, and the dopant inclusions are further confirmed by elemental analysis. Elemental analysis of K^+ ion-doped LTCA was carried out using EDAX analysis. Energy peaks correspond to different elements present in K^+ ion-doped L-threonine cadmium acetate are shown in Fig. 3. From the energy peaks, it was confirmed that K^+ metal ions were successfully incorporated in the crystal lattice of L-threonine cadmium acetate. The composition of elements and percentage of atoms present in the doped compound are given in Table 1. The potassium/cadmium (K/Cd) stoichiometric ratio obtained from the table is 0.3467 and the calculated

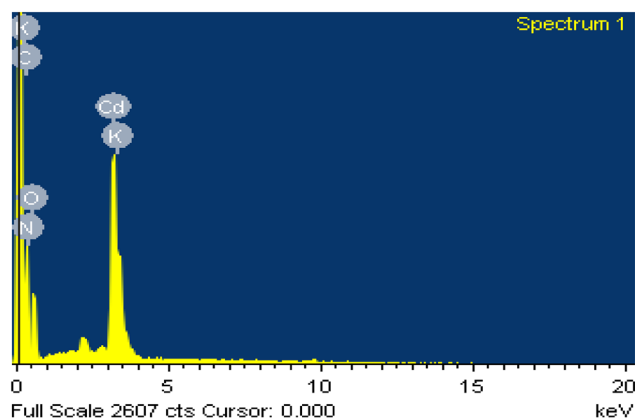
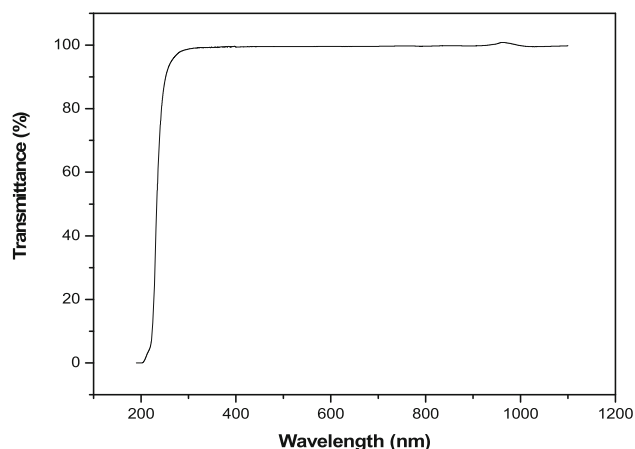


Fig. 3 EDAX spectrum of K^+ ion-doped LTCA

Table 1 Elemental Composition of K⁺ ion-doped LTCA

Element	Series	Unn (wt%)	C norm (wt%)	C atom (at %)	C error (wt% sigma)
C	K	39.97	31.39	47.89	2.13
N	K	1.70	9.27	12.13	3.12
O	K	10.66	30.64	35.10	1.64
K	K	0.73	0.68	0.32	0.20
Cd	L	22.63	28.01	4.57	1.34

**Fig. 4** Transmission spectrum of K⁺ ion-doped LTCA

stoichiometric applied in the preparation process of potassium-doped LTCA is 0.3478.

Figure 4 depicts the optical transmission spectrum for a crystal of 3.14 mm thick L-threonine cadmium acetate that has been doped with K⁺. Table 2 displays the estimated optical parameters. From the spectrum, it was confirmed that the crystal has lower cutoff wavelengths of 230.35 nm. Pure LTCA shows around 60% of transmittance [11]; after doping, the transmittance percentage increases and the lower cutoff wavelength of potassium-doped compound shifts near the UV region which is mainly due to the mesmeric effect arising between the pi bond and the lone pair of electrons in the orbital. Good percentage of optical transmittance of K⁺-doped LTCA crystal can be used in energy conversion devices, optical filters, and optoelectronic device applications. The delocalization of electron orbital in K⁺ ion-doped L-threonine cadmium acetate is mainly considered for nonlinear optical response [23, 24]. Higher transmittance percentage leads to higher electron affinity of potassium metal compared to cadmium crystal elucidate that the synthesized crystal can be used as filter for UV light in the wavelength range between 250 and 1100 nm [25].

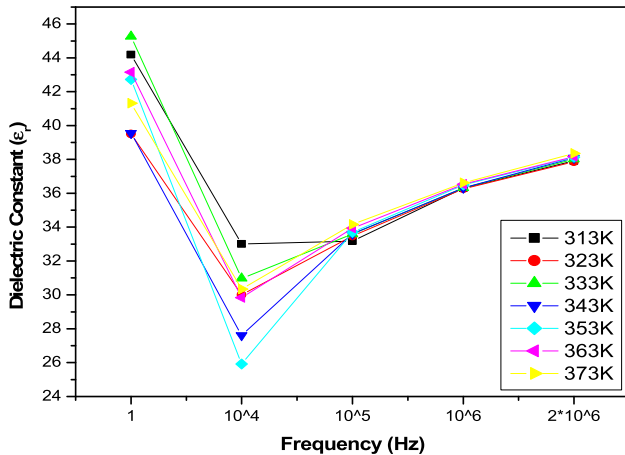
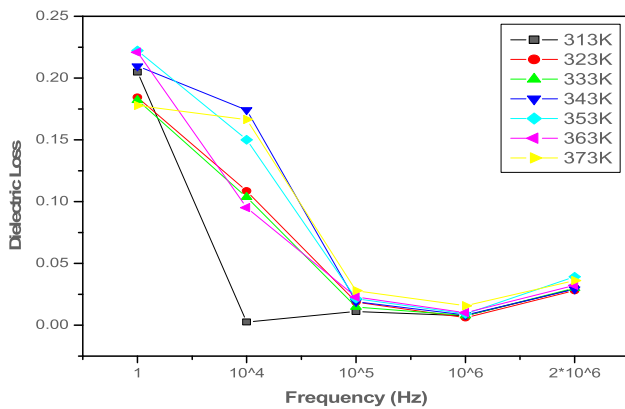
The calculated valance and conduction band edge shows that the energy bandgap is found to be higher in the order of 5.092 eV which is considered as insulators. Dielectric materials have wide industrial applications in optoelectronic industry and capacitors. Monoclinic crystal with greater refractive index of potassium-doped crystal is mainly suitable for prism fabrications.

In order to study the dielectric properties of the synthesized crystal, the calculated static permittivity as a function of frequency measured is shown in Fig. 5. Organometallic compound shows very interesting dielectric properties due to the presence of organic frame which can be utilized as temporary batteries in automobiles. As the frequency applied for K⁺-doped LTCA crystal increases, the static permittivity decreases initially then increases and the maximum value of dielectric constant experienced at lower frequency. Therefore, the organometallic compound can be used as energy storage materials at the lower-frequency region. In the crystal system, polarizations are mainly due to electronic, ionic, and orientation. Electronic polarization is due to the displacement of positive charge nucleus and electrons in opposite direction when the field is applied. Ionic polarization is caused due to the shift of Cd²⁺, K⁺, C₂H₃O₂⁻, and C₄H₈NO₃⁻ ions. The static permittivity decreases with increase in frequency and a sudden drop of frequency at 10⁴ Hz is due to the property that dipoles cannot orient themselves because of the acetate molecules present in the dopant. The orientation polarization arises due to the presence of H₂O molecules present in the crystal. Due to the asymmetric charge distribution, secondary bonds arise between the amino and acetate group present in the crystal.

Frequency-dependent dielectric loss of K⁺ ion-doped LTCA is shown in Fig. 6. It was noticed that, as the frequency increases, dielectric loss decreases up to 10 kHz and then increases for 313 K. The maximum value of dielectric losses was experienced at

Table 2 Calculated optical parameters of K⁺-doped crystal

Absolute electronegativity (χ)	$E_{(CB)}$ (eV)	$E_{(VB)}$ (eV)	Extinction coefficient	Reflectance	Refractive index	Electrical susceptibility	Electronic polarization (cm^3)
7.026	- 0.02	5.072	0.2347	1.30	5.41	2.2462	2.132×10^{-23}

**Fig. 5** Frequency Vs dielectric constant of K⁺ ion-doped LTCA**Fig. 6** Frequency Vs dielectric loss of K⁺ ion-doped LTCA

lower frequency. The dielectric loss increases with increase in temperature is ascribed due to the presence of space charge polarization near the grain boundary interfaces [26, 27]. It was interesting to report that the value of dielectric constant and dielectric loss decreases and attains lower minimum and then increases. In K⁺ ion-doped LTCA, the lowest minimum position shifts toward the higher-frequency range and experiences high static permittivity and low dielectric loss; this is mainly due to the influence of potassium (1.51 Å) with higher ionic radii and high degree of reactivity compared to the

Table 3 Calculated values of K⁺ ion-doped LTCA crystal

Parameters	Value
Plasma energy (eV)	29.19687
Penn gap (eV)	4.39162
Fermi gap (eV)	26.5038
Fermi velocity (m/s)	3.05×10^6
Fermi temperature (K)	30.7290×10^4
Polarization (cm^3) Penn analysis	4.386×10^{-23}
Polarization (cm^3) Clausius–Mossotti equation	4.381×10^{-23}

LTCA crystal lattice with cadmium (0.95 Å). Thus, potassium-doped crystal experiences polar dielectric nature having finite dipole in the absence of electric field. This property can be utilized for high-power electrical applications such as display, energy storage in high-frequency electronic circuits and dielectric filters [27].

Using the dielectric measurements, the theoretically calculated parameters are tabulated (Table 3). It was confirmed that due to doping plasma energy, Fermi gap, Fermi voltage, and Fermi temperature increase which proved that the material has higher electronic energy. Due to the doping of K⁺ ions, polarization of the potassium-doped LTCA compound decreases, which leads to lower activation energy because of the larger covalent radius of potassium compared to pure cadmium [28, 29]. Thus, for the greater value of plasma energy and the Fermi gap, the prepared K⁺-doped crystal with organic ligands modifies the dielectrical properties of the crystal which are highly recommended for dielectric filters.

Figure 7 depicted the recorded TG/DTA curve; there is no change in the weight loss up to 120 °C; therefore, the grown crystal can be exploited for optical and dielectric application up to 125 °C. Pure LTCA material is thermally stable up to 105 °C, as the doping temperature increases nearly 15 °C. From the TG/DTA curve, the initial weight 11.06% of the sample occurred due to two water molecules in the

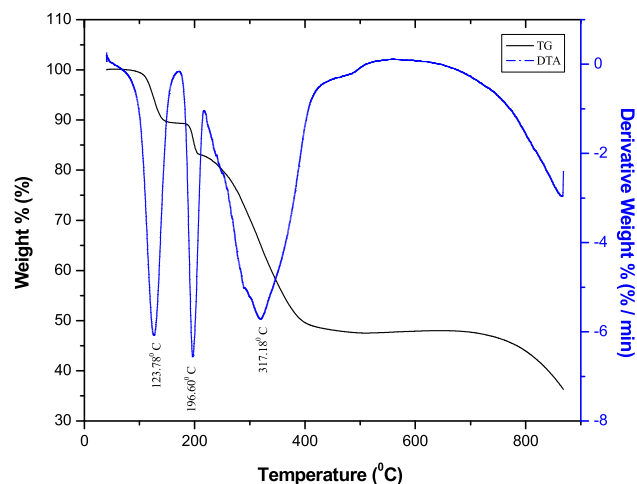


Fig. 7 TG/DTA curve of K^+ ion-doped LTCA

cadmium acetate dihydrate. The second stage of weight loss was found to be about 8% corresponding to the decomposition of carbon molecule. The major weight loss of about 36% is due to the liberation of $C_4H_7NO_3$. This is followed by the liberation of CH_6 corresponds to the final weight loss of about 6%.

The magnetic nature of the grown crystal is studied from the field Vs moment graph (Fig. 8). Pure [11] and K^+ ion-doped LTCA shows diamagnetic behavior due to the completely filled electron in s-shell. When an external magnetic field is applied, they are slightly repelled by an external magnetic field with saturated magnetization of $552.21E^{-6}$ emu, negative coercivity of 227.45G, and retentivity of $16.647E^{-6}$ emu. The main application of diamagnetic organometallic material is to stimulate microgravity environments in a sensors, actuators, and accelerometers [30].

The second harmonic output of potassium-doped LTCA was obtained by irradiating a pulsed laser beam. The source of Nd-YAG laser with a pulse width of 6 ns, pulse energy of 0.70 J, and repetition rate of 10 Hz. The powdered form of Potassium Dihydrogen Phosphate (KDP) was used as a reference and the SHG conversion efficiency of KDP is 8.94 mV and K^+ ion-doped LTCA is 5.26 mV. It was found that the SHG conversion efficiency of potassium-doped LTCA was found to be 59% (for pure 40% compared to KDP). The increase in SHG efficiency is due to the variation in the electronic configuration of the K^+ on and Cd^{2+} metal ion. Due to partially filled electron in potassium, when the laser

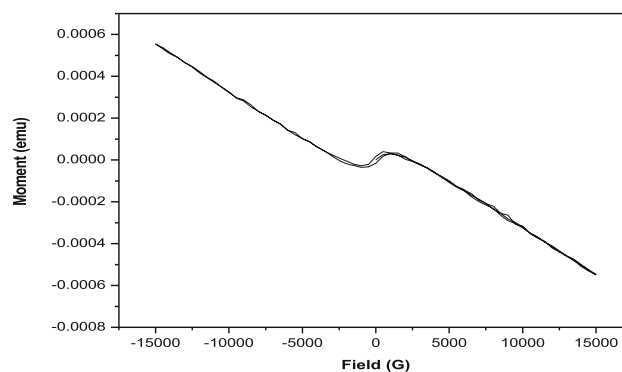


Fig. 8 Field Vs Moment graph of K^+ ion-doped LTCA

pulse interacts with the sample, they are easily polarized hence the efficiency increases.

4 Conclusion

Organometallic compounds provide a diverse platform for the development of dielectric materials for energy storage batteries, gate transistors, filters, and potential biological uses. K^+ ions integrated LTCA single crystal with a monoclinic crystal structure formed by a simple slow evaporation crystal growth technique. The asymmetric unit of polymeric structure experiences a linear two-fold configuration with two ligancies. The presence of potassium dopants was confirmed using EDAX analysis. Doping enhances the optical transmittance percentage of the crystal, making it acceptable for NLO and device construction. Dielectric studies reveal that doping potassium metals with a more covalent and ionic nature improves ionic polarization. The calculated dielectric parameters proved that the hybrid metal organic frame tuned by the K^+ ion plays an important role in the use of solid-state bioelectrical materials for various engineering applications such as dielectric filters. TG/DTA study witnessed that the potassium doping increases the stability of the crystal nearly $15^\circ C$. Magnetic studies confirm the diamagnetic nature of the grown crystal. The SHG conversion efficiency of potassium-doped LTCA crystal was found to be 59%. The expanded structural motif increases the impact of the potassium-doped LTCA compounds' linear and nonlinear optical, magnetic, thermal, and dielectric properties.

Author contributions

All authors contributed to the study conception and design. Material preparation data collection and analysis were performed by MAJQ, KCB, and PAU. The first draft of the manuscript was written by MAJQ and all the authors commented on the previous versions of the manuscript. MAJQ conceived and designed the analysis: designed the work plan, performed the analysis: synthesis of the compound, collected the data: the data were collected by characterization technique, and wrote the paper: manuscript was written. KCB: conceived and designed the analysis: designed the work plan, performed the analysis: helped to carry out the analysis, collected the data: the data were collected by characterization technique, and wrote the paper: suggestions were given and modified the content. PAU: conceived and designed the analysis: helped to design a work plan, performed the analysis: helped to carry out the analysis, and wrote the paper: suggestions were given and modified the content. All the authors read and approved the final manuscript.

Funding

This research received no specific grant from any funding agency.

Data availability

The datasets generated during and/or analyzed during the current study are available from the corresponding author on reasonable request.

Declarations

Competing interests The authors declare that they have no known competing financial interests or personal relationships that could have appeared to influence the work reported in this paper.

Research involving human and/or animal participants This article does not contain any studies involving human participants or animals performed by any of the authors.

References

1. G.D. Batema, C.A. van Walree, G.P. van Klink, C. de Mello Donegá, A. Meijerink, J. Perez-Moreno et al., *J. Organomet. Chem.* **867**, 246 (2018)
2. D. Banerjee (ed.), *Coordination chemistry* (Asian book private limited, New Delhi, 2009)
3. M.J. Rosker, P. Cunningham, M.D. Ewbank, H.O. Marcy, F.R. Vachss, L.F. Warren et al., *J. Eur. Opt. Soc.* **5**, 667 (1996)
4. K. Selvaraju, R. Valluvan, K. Kirubavathi, S. Kumararaman, *Opt. Commun.* **269**, 230 (2007)
5. L. Zhang, S. Revathi, in *Reference module in material science and materials engineering*, ed. by Caitlin Beddows (Elsevier, USA, 2016)
6. J. Peter, G. Mallard William, *NIST Chemistry web Book*, NIST Standard reference database number 69, Gaithersburg (1997)
7. M. Stoeppler (ed.), *Techniques and instrumentation in analytical chemistry* (Elsevier, USA, 1992)
8. S.K. Tilley, R.C. Fry (eds.), *Systems biology in toxicology and environmental health* (Elsevier, USA, 2015)
9. E.W.P. Wong, C.Y. Cheng (eds.), *Comprehensive Toxicology* (Elsevier, USA, 2010)
10. M. Abila Jeba Queen, K.C. Bright, S. Mary Delphine, *IUCr Data* **3**, x18177 (2018)
11. M. Abila Jeba Queen, K.C. Bright, S. Mary Delphine, P. Aji Udhaya, *Spectrochim Acta A Mol. Biomol. Spectrosc.* **228**, 117802 (2019)
12. M. Abila Jeba Queen, K.C. Bright, S. Mary Delphine, P. Aji Udhaya, *J. Mater. Sci. Mater. Electron.* **32**, 13261 (2021)
13. E.P. Wagner, *J. Chem. Educ.* **93**, 1289–1298 (2016)
14. Qi. Shao, H.L.M. Shao, *ACS Omega* **5**(18), 10297–10300 (2020)
15. B.B. Shabu, K.S. Shin, J.G. Han, *Plasma Sources Sci. Technol.* **25**, 015017 (2016)
16. T. Meyerhofer, J. Popp, *Spectrochim. Acta A Mol. Biomol. Spectrosc.* **191**, 121 (2017)
17. H. Mutschke, *Chem. Phys. Chem.* **17**, 13 (2016)
18. G. Marudhu, S. Krishnan, G.V. Vijayaragavan, *Optik* **125**, 2417–2421 (2014)
19. M. Shakir, S.K. Kushwaha, K.K. Maurya, R.C. Bhatt, W.M.A. Rashmi, G. Bhagavannarayana, *Mater. Chem. Phys.* **120**, 566–570 (2010)
20. P. Koteeswari, S. Suresh, P. Mani, *Am. J. Condensed Matter Phys.* **2**, 116–119 (2012)
21. E. Talebian, M. Talebian, *Optik* **124**, 2324–2326 (2013)
22. V. Rajendran (ed.), *Materials Science* (Tata McGraw-Hill Publishing Company Limited, New Delhi, 2011)
23. A.J. Shields, *Nat. Phot.* **1**, 215 (2007)

24. T.K. Kumar, S. Janarthanan, S. Pandi, M.V.A. Raj, J. Kana-galakshmi, D.P. Anand, JM MCE **9**, 961 (2010)
25. T. Kalaiarasi, M. Senthilkumar, S. Shanmugan, T. Jarin, V. Chithambaram, Bull. Mater Sci **44**, 175 (2021)
26. C.P. Smyth (ed.), *Dielectric Behaviour and Structure* (McGraw- Hill, New York, 1965)
27. K.C. Bright, T.H. Freeda, J. Appl. Phys. A. **99**, 935 (2010)
28. G.M. Matenoglou, L.E. Koutsokeras, E. Lekka Ch, G. Aba-dias, S. Camelio, G.A. Evangelakis et al., J. Appl. Phy. **104**, 124907 (2008)
29. A. Ben Rhaiem, F. Hlel, M. Guidara Kand Gargouri, J. Alloys Compd. **485**, 718 (2009)
30. F.G. Yuan (ed.), *Structural Health monitoring in aerospace structures* (Elsevier, USA, 2016)

Publisher's Note Springer Nature remains neutral with regard to jurisdictional claims in published maps and institutional affiliations.

Springer Nature or its licensor (e.g. a society or other partner) holds exclusive rights to this article under a publishing agreement with the author(s) or other rightsholder(s); author self-archiving of the accepted manuscript version of this article is solely governed by the terms of such publishing agreement and applicable law.